発表者氏名	論文タイトル名	発表誌名	巻号	ページ	出版年
俣野哲朗					
Moriya C, Horiba S, Inoue M, Iida A, Hara H, Shu T, Hasegawa M, Matano T	Antigen-specific T-cell induction by vaccination with a recombinant Sendai virus vector even in the presence of vector-specific neutralizing antibodies in rhesus macaques.	Biochem Biophys Res Commun	371	850-854	2008
Kawada M, Tsukamoto T, Yamamoto H, Iwamoto N, Kurihara K, Takeda A, Moriya C, Takeuchi H, Akari H, Matano T	Gag-specific cytotoxic T lymphocyte-based control of primary simian immunodeficiency virus replication in a vaccine trial.	J Virol	82	10199-10206	2008
高橋秀実					
Wakabayashi A, Nakagawa Y, Shimizu M, Moriya K, Nishiyama Y, Takahashi H.	Suppression of Already Established Tumor Growing through Activated Mucosal CTLs Induced by Oral Administration of Tumor Antigen with Cholera Toxin.	J Immunol	180	4000-4010	2008
Fukazawa Y, Miyake A, Ibuki K, Inaba K, Saito N, Motohara M, Horiuchi R, Himeno A, Matsuda K, Matsuyama M, Takahashi H, Hayami M, Igarashi T, Miura T.	Small intestine CD4+ T cells are profoundly depleted during acute simian-human immunodeficiency virus infection, regardless of viral pathogenicity	J Virol	82	6039-6044	2008
Yamashita T, Tamura H, Satoh C, Shinya E, Takahashi H, Chen L, Kondo A, Tsuji T, Dan K, Ogata K.	Functional B7.2 and B7-H2 molecules on myeloma cells are associated with a growth advantage.	Clin Cancer Res	15	770-777	2009
Higuchi T, Shimizu M, Owaki A, Takahashi M, Shinya E, Nishimura T, Takahashi H.	A possible mechanism of intravesical BCG therapy for human bladder carcinoma: involvement of innate effector cells for the inhibition of tumor growth.	Cancer Immunol Immunother	in press		2009
高橋秀実	免疫応答とエネルギーのめぐり.	癒しの環境	13 印刷中		2008
若林あや子、高橋秀実	ピロリ菌ウレアーゼによる B-1 細胞活性化作用と自己免疫疾患誘導の可能性.	日本栄養学会誌	印刷中		2008
高橋めぐみ、高橋秀実	遊離抗原による CD8+T 細胞のアポトーシス誘導.	臨床免疫・アレルギー科	印刷中		2008
高橋秀実	HIV に対する防御：細胞性免疫の役割.	治療学	印刷中		2008
高橋秀実	HIV 感染伝播における母乳中細胞の役割.	血液フロンティア	印刷中		2008

発表者氏名	論文タイトル名	発表誌名	巻号	ページ	出版年
満屋裕明					
Ghosh AK, Chapsal BD, Baldridge A, Ide K, Koh Y, Mitsuya H.	Design and Synthesis of Stereochemically Defined Novel Spirocyclic P2-Ligands for HIV-1 Protease Inhibitors.	Org Lett	10	5135-5138	2008
Ghosh AK, Gemma S, Takayama J, Baldridge A, Leshchenko-Yashchuk S, Miller HB, Wang YF, Kovalevsky AY, Koh Y, Weber IT, Mitsuya H.	Potent HIV-1 protease inhibitors incorporating meso-bicyclic urethanes as P2-ligands: structure-based design, synthesis, biological evaluation and protein-ligand X-ray studies.	Org Biomol Chem	6	3703-3713	2008
Ghosh AK, Gemma S, Baldridge A, Wang YF, Kovalevsky AY, Koh Y, Weber IT, Mitsuya H.	Flexible cyclic ethers/polyethers as novel P2-ligands for HIV-1 protease inhibitors: design, synthesis, biological evaluation, and protein-ligand X-ray studies.	J Med Chem	51	6021-6033	2008
Maeda K, Das D, Yin PD, Tsuchiya K, Ogata-Aoki H, Nakata H, Norman RB, Hackney LA, Takaoka Y, Mitsuya H.	Involvement of the second extracellular loop and transmembrane residues of CCR5 in inhibitor binding and HIV-1 fusion: insights into the mechanism of allosteric inhibition.	J Mol Biol	381	956-974	2008
Kawamoto A, Kodama E, Sarafianos SG, Sakagami Y, Kohgo S, Kitano K, Ashida N, Iwai Y, Hayakawa H, Nakata H, Mitsuya H, Arnold E, Matsuoka M.	2'-deoxy-4'-C-ethynyl-2-halo-adenosines active against drug-resistant human immunodeficiency virus type 1 variants.	Int J Biochem Cell Biol	40	2410-2420	2008
Nakata H, Steinberg SM, Koh Y, Maeda K, Takaoka Y, Tamamura H, Fujii N, Mitsuya H.	Potent synergistic anti-human immunodeficiency virus (HIV) effects using combinations of the CCR5 inhibitor aplaviroc with other anti-HIV drugs.	Antimicrob Agents Chemother	52	2111-2119	2008
Ghosh AK, Chapsal BD, Weber IT, Mitsuya H.	Design of HIV Protease Inhibitors Targeting Protein Backbone: An Effective Strategy for Combating Drug Resistance.	Acc Chem Res	41(1)	78-86	2008
Mitsuya H, Maeda K, Das D, Ghosh AK.	Development of protease inhibitors and the fight with drug-resistant HIV-1 variants.	Adv Pharmacol	56	169-197	2008
Koh Y, Das D, Leschenko S, Nakata H, Ogata-Aoki H, Amano M, Nakayama M, Ghosh AK, Mitsuya H.	GRL-02031: A Novel Nonpeptidic Protease Inhibitor (PI) Containing A Stereochemically Defined Fused Cyclopentanyltetrahydrofuran (Cp-THF) Potent Against Multi-PI-Resistant HIV-1 In Vitro.	Antimicrob Agents Chemother	53	997-1006	2009

発表者氏名	論文タイトル名	発表誌名	巻号	ページ	出版年
Aoki M, Venzon DJ, Koh Y, Aoki-Ogata H, Miyakawa T, Yoshimura K, Maeda K, Mitsuya H.	Non-cleavage Site Gag Mutations in Amprenavir-resistant HIV-1 Predispose HIV-1 to Rapid Acquisition of Amprenavir Resistance But Delays Development of Resistance to Other Protease Inhibitors.	J Virol	Epub ahead of print		2009
岩本愛吉					
Komuro I, Sunazuka T, Akagawa KS, Yokota Y, Iwamoto A, Omura S	Erythromycin derivatives inhibit HIV-1 replication in macrophages through modulation of MAPK activity to induce small isoforms of C/EBPbeta.	Proc Natl Acad Sci USA	105 (34)	12509-12514	2008
Mizukoshi F, Yamamoto T, Mitsuki YY, Terahara K, Kawana-Tachikawa A, Kobayashi K, Iwamoto A, Morikawa Y, Tsunetsugu-Yokota Y.	Activation of HIV-1 Gag-specific CD8(+) T cells by yeast-derived VLP-pulsed dendritic cells is influenced by the level of mannose on the VLP antigen.	Microbes Infect	11(2)	191-197	2009
Miyazaki E, Kawana-Tachikawa A, Tomizawa M, Nunoya J, Odawara T, Fujii T, Shi Y, Gao GF, Iwamoto A.	Highly restricted T-cell receptor repertoire in the CD8+ T-cell response against an HIV-1 epitope with a stereotypic amino acid substitution.	AIDS	23(6)	651-660	2009
清野　宏					
Kunisawa J, Gohda M, Kurashima Y, Ishikawa I, Higuchi M, and Kiyono H.	Sphingosine -phosphate-dependent trafficking of peritoneal B cells requires functional NFκB-inducing kinase in stromal cells.	Blood	111	4646-4652	2008
Gohda M, Kunisawa J, Miura F, Kagiyama Y, Kurashima Y, Higuchi M, Ishikawa I, Ogahara I, and Kiyono H	Sphingosine 1-phosphate regulates the egress of IgA plasmablasts from Peyer's patches for intestinal IgA responses.	J Immunol	180	5335-5343	2008
Terahara T, Igarashi O, Yoshida M, Nochi T, Kurokawa S, Takayama N, Yuki Y, Low AW, and Kiyono H.	Comprehensive gene expression analysis among Peyer's patch M cells, villous M cells and intestinal epithelial cells by DNA microarray analysis.	J Immunol	180	7840-7846	2008
Chang SY, Cha HR, Uematsu S, Akira S, Igarashi O, Kiyono H,and Kweon MN	Colonic patches direct the cross-talk between systemic compartments and large intestine independently of innate immunity.	J Immunol	180	1609-1618	2008
Chang SY, Cha HR, Igarashi O, Rennert PD, Kissenpfennig A, Malissen B, Nanno M, Kiyono H, and Kweon MN.	Cutting edge: Langerin+ dendritic cells in the mesenteric lymph node set the stage for skin and gut immune system cross-talk.	J Immunol	180	4361-4365	2008

発表者氏名	論文タイトル名	発表誌名	巻号	ページ	出版年
Uematsu S, Fujimoto K, Jang MH, Yang BG, Jung YJ, Nishiyama M, Sato S, Tsujimura T, Yamamoto M, Yokota Y, Kiyono H, Miyasaka M, Ishii KJ, and Akira S.	Regulation of humoral and cellular gut immunity by lamina propria dendritic cells expressing Toll-like receptor 5.	Nat Immunol	9	769-776	2008
Hashizume T, Togawa A, Nochi T, Igarashi O, Kweon MN, Kiyono H, and Yamamoto M.	Peyer's patches are required for intestinal IgA responses to *Salmonella*.	Infect Immun	76	927-934	2008
Momoi F, Hashizume T, Kurita-Ochiai T, Yuki Y, Kiyono H, and Yamamoto M.	Nasal vaccination with the 40-kilodalton outer membrane protein of *porphyromonas gingivalis* and a nontoxic chimeric enterotoxin adjuvant induces lomg-term protective immunity with reduced levels of immunoglobulin E antibodies.	Infect Immun	76	2777-2784	2008
Kunisawa J, Nochi T, and Kiyono H.	Immunological commonalities and distinctions between airway and digestive immunity.	Trends Immunol	29	505-513	2008
Fehervari1 Z, and Kiyono H.	The mucosa: at the frontlines of immunity.	Trends Immuno	29	503-504	2008
駒野　淳					
Urano E, Kariya Y, Futahashi Y, Ichikawa R, Hamatake M, Fukazawa H, Morikawa Y, Yoshida T, Koyanagi Y, Yamamoto N, Komano J.	Identification of the P-TEFb complex-interacting domain of Brd4 as an inhibitor of HIV-1 replication by functional cDNA library screening in MT-4 cells.	FEBS Let	582 (29)	4053-4058	2008
Urano E, Aoki T, Futahashi Y, Murakami T, Morikawa Y, Yamamoto N, Komano J.	Substitution of the myristoylation signal of human immunodeficiency vius type 1 Pr55Gag with the phospholipase C delta 1 pleckstrin homology domain results in infectious pseudovirion production.	J Gen Virol	89 (Pt12)	3144-3149	2008
Urano E, Shimizu S, Futahashi Y, Hamatake M, Morikawa Y, Takahashi N, Fukazawa H, Yamamoto N, Komano J.	Cyclin K/CPR4 inhibits primate lentiviral replication by inactivating Tat/positive transcription elongation factor b-dependent long terminal repeat transcription.	AIDS	22(9)	1081-1083	2008
Yoshida T, Kawano Y, Sato K, Ando Y, Aoki J, Miura Y, Komano J, Tanaka Y, Koyanagi Y.	A CD63 mutant inhibits T-cell tropic human immunodeficiency virus type 1 entry by disrupting CXCR4 trafficking to the plasma membrane.	Traffic	9(4)	540-558	2008

発表者氏名	論文タイトル名	発表誌名	巻号	ページ	出版年
Fuji H, Urano E, Futahashi Y, Hamatake M, Tatsumi J, Hoshino T, Morikawa Y, Yamamoto N, Komano J.	Derivatives of 5-nitro-furan-2-carboxylic acid carbamoylmethyl ester inhibit RNase H activity associated with HIV-1 reverse transcriptase.	J Med Chem	in press		2009
Hamatake M, Aoki T, Futahashi Y, Urano E, Yamamoto N, Komano J.	Ligand-independent higher-order multimerization of CXCR4, a G-protein-coupled chemokine receptor involved in the targeted metastasis.	Cancer Sci	in press		2009

Ⅳ. 研究成果の刊行物・別刷（抜粋）

doi: 10.1111/j.1365-3083.2008.02168.x

Mucosal Administration of Completely Non-Replicative Vaccinia Virus Recombinant Dairen I strain Elicits Effective Mucosal and Systemic Immunity

N. Yoshino*,†, M. Kanekiyo†, Y. Hagiwara‡, T. Okamura†, K. Someya†, K. Matsuo†, Y. Ami§, S. Sato*, N. Yamamoto† & M. Honda†

*Department of Microbiology, School of Medicine, Iwate Medical University, Iwate; †AIDS Research Center, National Institute of Infectious Diseases, Tokyo; ‡Research Center for Biologicals, The Kitasato Institute, Saitama; and §Division of Experimental Animals Research, National Institute of Infectious Diseases, Tokyo, Japan

Received 27 March 2008; Accepted in revised form 15 July 2008

Correspondence to: N. Yoshino, Department of Microbiology, School of Medicine, Iwate Medical University, 19-1 Uchimaru, Morioka, Iwate 020-8505, Japan. E-mail: nyoshino@iwate-med.ac.jp

Abstract

We studied the immunogenicity of completely replication-deficient vaccinia virus Dairen I strain recombinant encoding simian immunodeficiency virus (SIV) *gag/pol* (rDIs) in both mucosal and systemic compartments. When administered either intranasally or intragastrically, rDIs elicited enhanced levels of both SIV Gag p27-specific IgA antibodies and specific plasma antibodies, and the enhanced immunity persisted for the 1-year of observation by intranasal immunization. Increases were observed in antigen-specific IgA antibody-forming cells (AFC) in intestinal mucosal tissues and in IgG AFC in spleens. Furthermore, induction of type 1 and 2 helper cytokines in $CD4^+$ spleen T cells and of $CD8^+$ IFN-γ spot-forming cells in mucosal tissues was observed in the intranasally immunized mice. Moreover, not even high-dose rDIs generated an *SIV* gene signal in the brain tissues of immunized mice. These findings suggest that mucosal immunization with the DIs recombinant hold promise as a safe mucosal vector.

Introduction

Human immunodeficiency virus type-1 (HIV-1), like most infectious agents, gains entry into the host via the mucosal surfaces. Immunoprophylaxis by the mucosal route is an important approach to control mucosally transmitted infections. Moreover, because most generic immunization procedures for vaccinia virus require needles, mucosal vaccines pose the risk of cross-contamination due to needle reuse. But mucosal immunization would eliminate such a risk.

A number of groups have demonstrated the efficacy of poxvirus as a mucosal vaccine vector. Recombinant modified vaccinia virus Ankara (rMVA) expressing HIV-1 89.6 gp160 induced both mucosal and systemic cytotoxic T-lymphocyte responses in intrarectally immunized mice [1]. The MVA vector was tested in multiple prime-boost vaccine protection studies in macaques [2, 3]. In another study, NYVAC/SIV_{gpe}, the highly attenuated poxvirus vector NYVAC, encoding the SIV_{mak6w} *gag*, *pol*, and *env*, was administered via various routes and its immunogenicity against simian immunodeficiency virus (SIV) Gag peptide was assessed. This NYVAC study found that mucosal immunization routes were effective in inducing mucosal immune responses [4]. Obtaining the appropriate balance between safety and immunogenicity is a critical issue for the development of any vaccine. Some of vector systems, such as those based on replication-deficient poxviruses, are readily established and have undergone clinical testing in humans, mainly for safety and, to some extent, for immunogenicity [5–7].

In this study, we selected the completely replication-deficient vaccinia virus, Dairen I strain (DIs) for the vaccinia vector. A highly attenuated mutant of vaccinia virus obtained by successive 1-day egg passages of the DIE virus [8–10], DIs replicates only in chick embryo fibroblast cells and is not pathogenic to mice, guinea pigs or rabbits [8]. Although completely non-virulent, the recombinant virus efficiently produces foreign gene products [11, 12]. When systemically administered,

recombinants of DIs have induced specific immunities in mice and non-human primates [11–14]. Furthermore, the efficacy of prime-boost regimen that primed with recombinant *Mycobacterium bovis* bacillus Calmette-Guérin expressing SIV *gag* or DNA encoding SIV *gag* and *pol* genes and boosted by DIs recombinants have been shown in macaques [13, 14].

Although parenterally administered vaccines induce protective immune responses, they are less able to induce the mucosal immune responses needed to prevent infection at the site of initial contact between the host and the infectious agent [15]. However, no study has as yet been performed to determine the potential of recombinant DIs (rDIs) as a mucosal vaccine vector in experimental animals. In this study, we assessed the capability of rDIs to induce mucosal and systemic immunity in animals.

Materials and methods

Recombinant vaccinia virus vectors. We propagated rDIsSIV*gag/pol* as a candidate vaccine expressing full-length SIV *gag* and rDIs expressing LacZ (rDIsLacZ) as a control vector in chick embryo fibroblast cells and prepared them as previously described [11, 12]. Dr Bernard Moss (Laboratory of Viral Diseases, National Institute of Allergy and Infectious Diseases, National Institutes of Health, Bethesda, MD, USA) generously supplied the recombinant modified vaccinia virus Ankara (rMVA) expressing SIV *gag* (rMVA-SIV*gag/pol*) and non-recombinant MVA 74LVD6 as the parent strain of rMVA-SIV*gag/pol*. These vaccinia virus vectors were stored at −80 °C until used.

Mice. Five-week-old C57BL/6 mice (H-2^b) were purchased from Charles River Japan, Inc. (Yokohama, Japan). Mice were acclimated to the experimental animal facility for 1 week before being used in experiments and were maintained in the facility under pathogen-free conditions. All experimental procedures were conducted following the guidelines established by the National Institute of Infectious Diseases, Japan. The study was conducted in a biosafety-level 2 facility with the approval of an institutional committee for biosafety and in accordance with the requirements of the World Health Organization.

Immunization of mice. Several groups of mice were immunized with rDIsSIV*gag/pol* by intranasal, intragastrical or intradermal routes. Similar results were obtained when experiments were conducted for a second or third time. For intranasal immunization, the mice were lightly anesthetized with ketamine before being immunized with a 5-μl aliquot (2.5 μl/nostril) of PBS containing several concentrations of rDIsSIV*gag/pol*, rDIsLacZ, rMVA-SIV*gag/pol* or MVA 74LVD6. For intragastrical immunization, mice were deprived of food for 12 h before immunization and neutralized stomach acidity [16]. The mice were immunized with a 250-μl aliquot of PBS containing several concentrations of rDIsSIV*gag/pol* by intragastrical gavage. For intradermal immunization, the mice were lightly anesthetized with ketamine and immunized with a 50-μl aliquot of PBS containing several concentrations of rDIsSIV*gag/pol* in the inguinal region.

Sampling of plasma and fecal pellets. Blood and fecal pellets were collected 1 week after the last immunization, and then at 2 to 8-week intervals for 49 weeks. The collection and preparation methods have been previously described [17]. Samples of plasma and fecal extract were stored at −80 °C until needed.

Detection of p27-specific antibody production by enzyme-linked immunosorbent assay. Simian immunodeficiency virus Gag p27-specific antibody (Ab) titres in plasma and fecal extracts were determined by an endpoint enzyme-linked immunosorbent assay (ELISA). The assay was conducted in 96-well plates (Nalge Nunc International, Rochester, NY, USA), that had been coated with 1 μg/ml of SIV Gag p27 (recombinant Gag p27 SIV_{mac251}; ImmunoDiagnostics, Inc., Woburn, MA, USA) in PBS. Twofold serial dilutions of samples were added after blocking with 1% BSA–PBS. Horseradish peroxidase-conjugated goat anti-mouse IgG (H + L), IgM, or IgA Ab (Southern Biotechnology Associates, Inc., Birmingham, AL, USA) were used to detect the p27-specific Ab, which were then developed at room temperature with TMB+ substrate-chromogen (DAKO, Carpinteria, CA, USA). Endpoint titres were expressed as the last dilution that gave an optical density at 450 nm (OD_{450}) of ≥ 0.1 OD units above the OD_{450} of negative controls after 15-minute incubation. Incubations were terminated by addition of 0.5 M H_2SO_4.

Preparation of single-cell suspensions. Single-cell suspensions were obtained from spleen, submandibular lymph nodes (SMLN), mesenteric lymph nodes (MLN), Peyer's patches (PP), small intestinal lamina propria (i-LP), small intestinal intraepithelial lymphocytes (IEL), nasal lamina propria (n-LP), and nasopharynx-associated lymphoid tissue (NALT) ,and then prepared according to the protocols described elsewhere [17]. The cells were washed and resuspended in RPMI 1640 supplemented with 10% heat-inactivated fetal calf serum, antibiotics and 55 μM 2-mercaptoethanol (Sigma-Aldrich Co., St Louis, MO, USA) (complete medium).

Detection of p27-specific Ab-forming cells by enzyme-linked immuno spot assay. Simian immunodeficiency virus p27-specific IgG, IgM and IgA Ab-forming cells (AFC) in the mucosal and systemic tissues of mice were determined by enzyme-linked immuno spot (ELISPOT) assay which was conducted in 96-well filter plates (Millititer HA; Millipore Co., Bedford, MA, USA). Plates were coated with 1 μg/ml of SIV p27 in PBS. After blocking with complete medium, single-cell suspensions of mononuclear

cells from the spleen, MLN, PP, i-LP, n-LP and NALT were added at various concentrations into each well and incubated for 4 hours at 37 °C in 5% CO_2. SIV p27-specific AFC were detected by alkaline phosphatase-conjugated goat anti-mouse IgG (H + L), IgM or IgA Ab and developed with Nitro blue tetrazolium chloride/5-Bromo-4-chloro-3-indolyl phosphate, toluidine salt (Roche Diagnostics GmbH, Penzberg, Germany). After being washed with water, the palates were dried and p27-specific AFC were quantitated with the aid of stereomicroscope.

Analysis of the cytokine production of SIV Gag peptide-specific CD4⁺ T cells. $CD4^+$ T cells were isolated from spleen by auto MACS (Miltenyi Biotec GmbH, Bergisch Gladbach, Germany). The purified T-cell fractions were > 97% $CD4^+$ and were > 99% viable. Cells were resuspended in complete medium, and purified $CD4^+$ T cells (4×10^6 cells/ml) were cultured with or without 50 μg/ml of overlapping Gag peptides [12] in the presence of T cell-depleted, mitomycin C-treated splenic antigen-presenting cells (APC) at 37 °C in 5% CO_2. Culture supernatants were collected after 5 days, and IFN-γ, IL-4 and IL-10 were measured by ELISA kit (eBioscience, San Diego, CA, USA). The levels of Gag-specific cytokine production were calculated by subtracting the results of control cultures (e.g. without Gag peptide stimulation) from those of Gag peptide-stimulated cultures.

Analysis of IFN-γ production of SIV Gag peptide-specific CD8⁺ T cells. To prepare APC for this assay, $CD11c^+$ dendritic cells were isolated from the spleens of naive mice by auto MACS and then resuspended into complete medium before being added into 96-well anti-mouse IFN-γ Ab-coated (R&D Systems, Inc., Minneapolis, MN, USA), sterilized nitrocellulose plates at the rate of 1×10^4 APC/well. The APC were then incubated with or without 50 μg/ml of overlapping Gag peptides for 24 hours at 37 °C in 5% CO_2. $CD8^+$ T cells were isolated from spleen, SMLN, PP, and IEL by auto MACS. The enriched $CD8^+$ cells were added to APC-cultured wells and incubated for 24 hours at 37 °C in 5% CO_2. IFN-γ spot-forming cells (SFC) were detected by ELISPOT kit (R&D Systems, Inc.) and quantitated with the aid of stereomicroscope. The number of Gag-specific IFN-γ SFC was calculated by subtracting the results of the control culture (e.g. without Gag peptide stimulation) from those of the peptide-stimulated culture. In contrast, the calculated numbers of Gag-specific IFN-γ SFC of naive mice were < $20/10^6$ cells.

Detection of rDIsSIVgag/pol in the central nervous system by nested reverse transcription PCR. To determine the dissemination of intranasally administered rDIsSIV*gag/pol* in the brain, a nested DNA-PCR and reverse transcription PCR (RT-PCR) were used to amplify a fragment of the SIV *gag* gene [18]. Mice were intranasally inoculated with 10^6 plaque-forming units (PFU) of rDIsSIV*gag/pol*. After 48 hours, brains were removed and the olfactory bulbs, cerebellum and cerebrum were sectioned. The DNA and mRNA were extracted from the olfactory bulbs, cerebellum and cerebrum by the DNeasy tissue kit (QIAGEN, KJ Venlo, The Netherlands) and the RNeasy mini kit (QIAGEN), respectively. RT-PCR was performed using One-Step RT-PCR kit (Takara Bio Inc., Shiga, Japan). Reverse transcription was carried out at 50 °C for 30 min with avian myeloblastosis virus reverse transcriptase. The initial and nested PCR protocols and the sequences of the primers have been described elsewhere [18]. After the second amplification, 10 μl of nested PCR-amplified product was run on 1.0% agarose gel, and DNA bands were visualized by staining with ethidium bromide. The lowest concentration of plasmid SIV DNA that could be detected with this PCR method in the first amplification with outer gag primer pair was 10^3 copies. Upon further amplification with nested/internal gag primers, a single copy of plasmid DNA could be routinely detected [18].

Statistical Analysis. The results are expressed as the mean + the standard deviation (SD). Normally distributed variables were compared by using the two-tailed Student's *t* test and non-normally distributed variables by the two-tailed Mann–Whitney *U*-test. Probability value of < 0.05 was considered significant.

Results

Induction of SIV p27-specific IgA Ab responses in mucosal secretions

We ran an endpoint ELISA to determine the levels of SIV p27-specific IgA Ab in the fecal extracts by collecting fecal pellets at 1 week after the last immunization. SIV p27-specific IgA Ab were detected in the fecal extracts from all mice that had been immunized intranasally with 10^6 PFU of rDIsSIV*gag/pol* and in seven of the eight (88%) mice given 10^5 PFU of rDIsSIV*gag/pol* (Fig. 1). In contrast, p27-specific IgA Ab were detected in the fecal extracts from five of eight (63%) mice given 10^6 PFU of rDIsSIV*gag/pol* intragastrically. As a reference, SIV p27-specific IgA Ab were also detected in the fecal extracts of mice immunized intranasally with 10^3–10^6 PFU of rMVA-SIV*gag/pol* (Fig. 1). The titres of p27-specific IgA Ab in fecal extracts of mice immunized intranasally with 10^6 PFU of rDIsSIV*gag/pol* were significantly higher than in those mice immunized intranasally with the same dose of rMVA-SIV*gag/pol* ($P = 0.026$). No SIV p27-specific IgA Ab were detected in the fecal extracts of controls immunized with either rDIsLacZ or MVA 74LVD6 (Fig. 1). These results show that mucosal vaccination with rDIsSIV*gag/pol* can induce antigen (Ag)-specific humoral immunity in mucosal compartment.

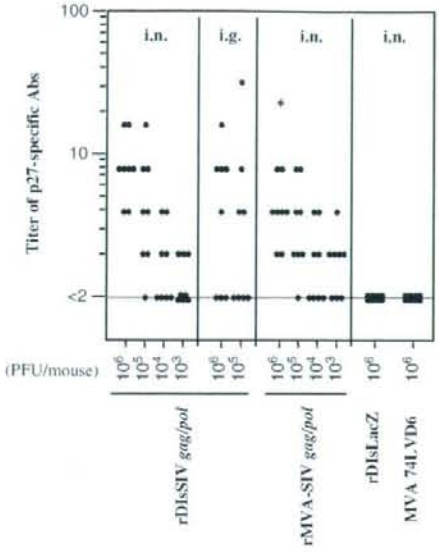

Figure 1 Titres of SIV p27-specific IgA Ab in fecal extracts of mice immunized with rDIsSIV*gag/pol* or rMVA-SIV*gag/pol*. Fecal pellets were collected at 1 week after the last immunization. The titres of p27-specific IgA Ab in the fecal extracts of mice immunized with rDIsSIV*gag/pol* or rMVA-SIV*gag/pol* were determined using an endpoint ELISA. The data are representative of two separate experiments. Each group was compared by a two-tailed Mann–Whitney *U*-test. Significant differences between rDIs group and rMVA group are indicated by asterisks (*$P < 0.05$). in, intranasal; ig, intragastrical.

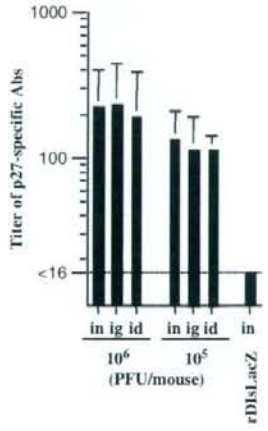

Figure 2 Comparison of SIV p27-specific IgG Ab responses in the plasma of mice immunized via different routes. Plasma samples were collected at 1 week after the last immunization. The titres of p27-specific IgG Ab in the plasma of mice immunized with 10^5 or 10^6 PFU of rDIsSIV*gag/pol* were determined using an endpoint ELISA. The data are shown as the mean titre + SD for 12 mice in each experimental group. Data are representative of three separate experiments. in, intranasal; ig, intragastrical; id, intradermal.

Induction of SIV p27-specific Ab in plasma of mice immunized via mucosal routes

Our previous studies showed that SIV Gag-specific immune responses were induced in mice intradermally immunized with rDIsSIV*gag/pol* [12]. We assessed that IgG Ab response to SIV p27 in the plasma of immunized mice at 1 week after the last immunization. Our results clearly show that intranasal, intragastrical, and intradermal immunization with rDIsSIV*gag/pol* induced p27-specific IgG Ab in plasma (Fig. 2), with similar titres of p27-specific IgG observed for intranasal, intragastrical and intradermal groups receiving the same dose. In contrast, the titres of < 16 were observed for p27-specific IgG Ab in plasma of control mice immunized intranasally with 10^6 PFU rDIsLacZ.

Induction of p27-specific AFC in the mucosal and systemic immune systems

Once the SIV p27-specific Ab responses had been further confirmed at the cellular level, we compared the number of p27-specific AFC induced in the mucosal and systemic lymphoid tissues after intranasal and intragastrical immunization with 10^5 PFU of rDIsSIV*gag/pol*. When we quantitated p27-specific AFC in the mucosal tissues and spleens of mucosally immunized mice, we found clear evidence of p27-specific IgA AFC in the PP, i-LP, NALT and n-LP of mice immunized intranasally with 10^5 PFU of rDIsSIV*gag/pol* (Fig. 3A). The numbers of p27-specific IgA AFC in the i-LP of intragastrically immunized mice were significantly higher than in intranasally immunized mice. Conversely, intranasal immunization of rDIsSIV*gag/pol* strongly induced p27-specific IgA AFC in the NALT and n-LP. We also found the number of p27-specific IgG AFC in the spleen of mice immunized intranasally with rDIsSIV*gag/pol* to be significantly higher than in intragastrically immunized mice ($P < 0.05$) (Fig. 3B). These findings suggest that mucosally administered rDIs can act as a vector for the induction of p27-specific AFC in both mucosal and systemic tissues.

Helper cytokine profiles of SIV Gag-specific CD4$^+$ T cells

Simian immunodeficiency virus Gag-specific helper T-cell responses were assessed using cytokine-specific ELISA for culture supernatants of CD4$^+$ T cells isolated from the spleen of immunized mice. Our results demonstrated that both type 1 helper T cell (Th1) and Th2 cytokines were upregulated in overlapping Gag peptide-stimulated CD4$^+$ T cells taken from the spleen of mice immunized with 10^5 PFU of rDIsSIV*gag/pol*. Of special note, the levels of IFN-γ in mice immunized intranasally with

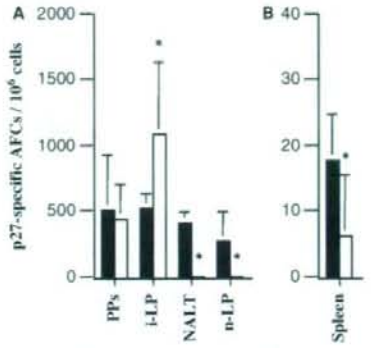

Figure 3 SIV p27-specific IgA AFC in the mucosal tissues and IgG AFC in systemic tissues of mice immunized intranasally or intragastrically with rDIsSIV*gag/pol*. The mice were killed 1 week after the last immunization. Levels of p27-specific IgA AFC in PP, i-LP, NALT and n-LP (A) and levels of p27-specific IgG AFC in spleen (B) of mice immunized intranasally (closed column) or intragastrically (open column) with 10^5 PFU rDIsSIV*gag/pol* were determined using an ELISPOT assay. The data are shown as the mean number of AFC/10^6 cells + SD for 12 mice in each experimental group. Data are representative of three separate experiments. Each group was compared by a two-tailed Student's *t* test. Significant differences between the intranasal group and intragastric group are indicated by asterisks (*$P < 0.05$).

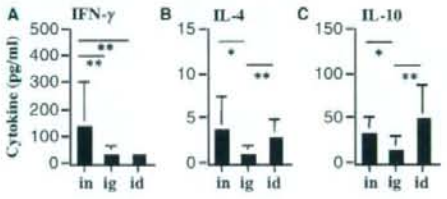

Figure 4 Th1/Th2 cytokine production of SIV Gag overlapping peptide-stimulated CD4$^+$ T cells of mice immunized with 10^5 PFU rDIsSIV*gag/pol*. CD4$^+$ T cells were isolated from spleen at 1 week after the last immunization. Culture supernatants were harvested and then analysed for the production of IFN-γ (A), IL-4 (B), and IL-10 (C) by ELISA. The levels of Gag-specific cytokine production were calculated by subtracting the results of the control culture from the peptide-stimulated culture. The data are shown as the mean concentration + SD for 12 mice in each experimental group. Data are representative of three separate experiments. Each group was compared by a two-tailed Student's *t* test. Significant differences are indicated by asterisks (*$P < 0.05$, **$P < 0.005$). in, intranasal; ig, intragastrical; id, intradermal.

rDIsSIV*gag/pol* were significantly higher than in those intragastrically or intradermally immunized (Fig. 4A). However, no preferential association was noted between Th2 and either the intranasal or intradermal group (Fig. 4B, 4C). In contrast, the intragastrical group showed significantly lower levels of Th2 cytokines than did the intranasal or intradermal group.

IFN-γ production of SIV Gag-specific CD8$^+$ T cells

Cytotoxic T-lymphocyte activity in viral infection has been shown to be of central importance for host defence. To assess the mucosal induction of cellular immunity, we assessed the CD8$^+$ IFN-γ -producing cells in the immunized mice. Because non-specific activated CD8$^+$ cells produced IFN-γ, the number of SIV Gag-specific IFN-γ SFC was calculated (see *Materials and methods*). In the IEL of mice immunized intranasally with rDIsSIV*gag/pol*, the numbers of IFN-γ SFC in unstimulated condition were 70–460 cells/10^6 CD8$^+$ cells. The numbers of IFN-γ SFC in Gag peptide-stimulated condition were 150–1385 cells/10^6 CD8$^+$ cells. There were significant differences between stimulated and unstimulated group. It was demonstrated that SIV Gag-specific IFN-γ-producing CD8$^+$ cells appeared in both systemic and mucosal compartments in the intranasally immunized mice and were particularly abundant in the IEL of the mice (Fig. 5).

Kinetics of p27-specific Ab in plasma

IgA, IgG and IgM class-specific endpoint ELISA was used to investigate an SIV p27-specific Ab in the plasma of mice immunized intranasally with 10^5 PFU of rDIsSIV*gag/pol*. Up until 11 weeks after the last immunization, the titres of p27-specific IgA Ab were low (mean values < 50). Without further boosting, increased p27-specific IgA Ab titres were observed after 11 weeks and were maintained in the plasma for approximately 1 year (49 weeks) at a mean value between 48 and 92 (Fig. 6A). Levels of p27-specific IgA Ab did not correlate with those of IgG and IgM Ab; p27-specific IgG Ab were maintained in the plasma for 1 year, and increases in IgG Ab titres were observed until 17–21 weeks after the last immunization. After peaking, the mean titre in

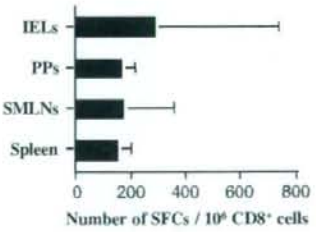

Figure 5 IFN-γ production of SIV Gag overlapping peptide-stimulated CD8$^+$ cells isolated from mucosal and systemic components of mice immunized with rDIsSIV*gag/pol*. CD8$^+$ cells were isolated from IEL, PP, SMLN and spleen at 1 week after the last immunization. IFN-γ production was assessed by ELISPOT assay. The number of Gag-specific IFN-γ SFC was calculated by subtracting the results of the control culture from those of the peptide-stimulated culture. The data are shown as the mean number of SFC + SD for 12 mice in each experimental group. Data are representative of three separate experiments.

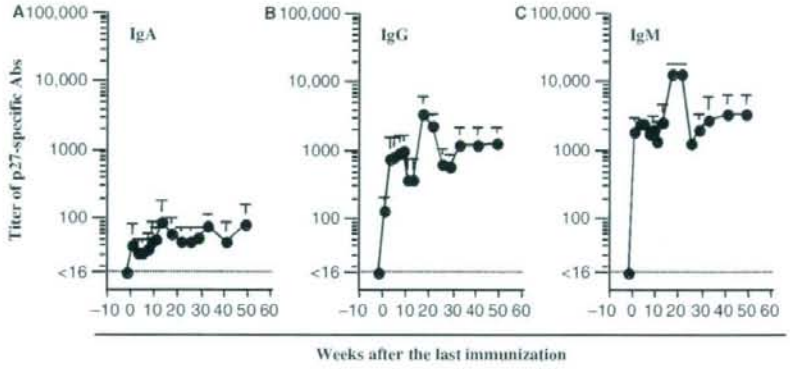

Figure 6 Sequential assessment of SIV p27-specific IgA, IgG, and IgM Ab in plasma of mice that have been intranasally immunized with 10^5 PFU rDIsSIV*gag/pol*. Plasma p27-specific IgA (A), IgG (B), and IgM (C) Ab were determined using an endpoint ELISA. The data are shown as the mean titres + SD for 12 mice in each experimental group. Data are representative of three separate experiments.

intranasally immunized mice declined to a value between 580 and 1300 (Fig. 6B). The p27-specific IgM Ab were observed in the plasma of intranasally immunized mice throughout the 1-year period (Fig. 6C). Titre kinetics was similar for p27-specific IgM Ab and IgG Ab. Thus, it is important to note that the p27-specific plasma Ab responses were maintained for 1 year after the last immunization via the nasal route.

We quantitated p27-specific IgG, IgM and IgA AFC both in systemic tissues such as spleen and in mucosal tissues such as MLN, PP, and i-LP of the mice at 49 weeks after the last immunization. Our results clearly demonstrated that high numbers of p27-specific IgG, IgM and IgA AFC in mice immunized intranasally with 10^5 PFU of rDIsSIV*gag/pol* were maintained even for 1 year after immunization (Fig. 7). Moreover, the mean titres of p27-specific IgA Ab in fecal extracts from mice at 49 weeks were 54 ± 18 (n = 12).

Analysis of viral dissemination in the central nervous system

Adverse reactions to vaccinia virus can occur regardless of pre-existing susceptibilities [19]. Of the adverse events known to occur after smallpox vaccination [20, 21], the most serious is post-vaccinal encephalitis (PVE) [20]. Although the pathogenesis of PVE is unknown, vaccinia viruses were isolated from brain tissues in PVE cases [22, 23]. As the nasopharynx resides in close proximity to the brain, we sought to determine whether rDI is disseminated from the nasal cavity to the brain. The olfactory bulbs, cerebellum and cerebrum of mice immunized intranasally with 10^6 PFU of rDIsSIV*gag/pol* were assessed using both nested DNA PCR and RT-PCR. The SIV *gag* gene was not detected in the olfactory bulbs, cerebellum or cerebrum of any of the eight mice (data not shown).

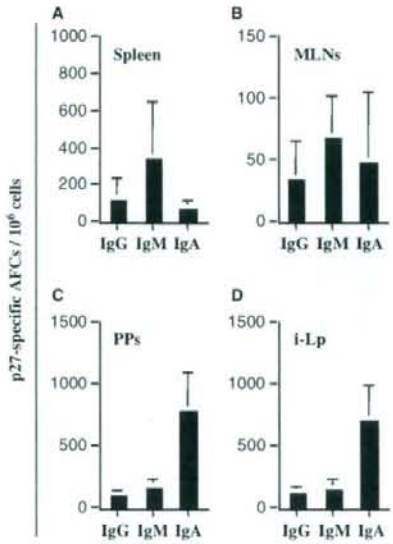

Figure 7 SIV p27-specific AFC in mucosal and systemic tissues of mice immunized intranasally with 10^5 PFU rDIsSIV*gag/pol* at 49 weeks after the last immunization. Levels of p27-specific IgG, IgM and IgA AFC in spleen (A), MLN (B), PP (C), and i-LP (D) of mice were determined using an ELISPOT assay. Data are shown as the mean number of AFC/10^6 cells + SD for 12 mice in each experimental group and the data are representative of three separate experiments.

Discussion

In this study, p27-specific IgA Ab in fecal extracts and IgG Ab in plasma were confirmed in mice immunized intranasally or intragastrically with rDIsSIV*gag/pol*. The compartmentalization within the mucosal immune system places constrains on the choice of vaccination route

for inducing effective immune responses. Oral immunization induces substantial Ab responses in the small intestine [24, 25]. We also found that the numbers of p27-specific IgA AFC were strongly induced in the small intestine by intragastrical route. Conversely, intranasal immunization results in Ab responses in the upper airway mucosa and regional secretions without evoking an immune response in the gut [26, 27]. Although the numbers of p27-specific IgA AFC in i-LP of mice intranasally immunized rDIsSIV*gag/pol* were significantly lower than intragastrical group, the titres of p27-specific IgA Ab in fecal extracts of mice immunized intranasally or intragastrically were roughly equivalent. Intranasal immunization of rDIsSIV*gag/pol* dominantly induced p27-specific IgA AFC in nasal tissues, and these cells might powerfully produce dimeric or polymeric IgA Ab. Polymeric IgA Ab removed from the circulation into bile by the hepatic polymeric immunoglobulin receptor/secretory component-driven. A large portion of murine gut IgA Ab is derived from blood rather than mucosal production [28–30]. Taken together, this study showed that intranasal immunization of rDIs, induced not only potent plasma IgA Ab response but also a good intestinal IgA Ab level despite a poorer cellular IgA Ab response in intestinal mucosa.

One of the keys to vaccine development is the longevity and stability of immune memory. We have shown that p27-specific IgG, IgM and IgA Ab and p27-specific AFC remain detectable for at least 1 year after intranasal administration of replication-deficient rDIsSIV*gag/pol*. Interestingly, IgM Ab against p27 in plasma were detected throughout the period of Ab monitoring, and significant numbers of p27-specific IgM AFC were observed in spleen even 1 year after immunization. Significantly more p27-specific IgM AFC were observed in spleens, suggesting that they may originate from those central lymphoid tissues in immunized mice. Based on the results of the current study, we theorize that SIV Gag continued to be produced in the mice in sufficient quantities to reactivate IgM Ab production in the absence of viral replication and reinfection. Others have shown that hepatitis B virus core Ag-specific or hepatitis C virus capsid Ag-specific IgM Ab are found in the plasma of individuals in the chronic phase of hepatitis B or C viral infection [31, 32]. We have not assessed long-term rDIs vector persistence in mucosal tissues, and we have not yet managed to elucidate the mechanism governing prolonged p27-specific Ab induction. However, we showed that rDIs were able to induce long-term immunity against an inserted foreign Ag in intranasally immunized mice.

Intranasal vaccination has caused unexpected complications. Although DIs vector did not detected in the brain of mouse in this study, it is not clear about the safety for human brain. Intranasal vaccination with rDIs may pose risks such as PVE. It must concern the possibility that nasal vaccines could enter the central nervous system, because of the anatomical proximity of the nasal cavity to the brain. On the other hand, although oral delivery has become an accepted route for administration of polio-vaccine, the gastrointestinal tract presents several formidable barriers to candidate vaccines. In general, oral immunization is relatively inefficient at evoking an IgA Ab response in the distal segments of the large intestine or female genital tract mucosa [24, 25]. Of special interest for possible vaccination against HIV and other sexually transmitted infections, not only intravaginal but also intranasal immunization has been found to give rise to substantial IgA and IgG Ab responses in human cervicovaginal mucosae [24, 27, 33]. This study demonstrated that both intranasal and intragastrical immunizations of rDIs induce Ag-specific mucosal immune responses. However, we could not settle which is the better strategy of vaccine administration to prevent HIV infection in this study.

Of course, much more intensive examination of the efficacy and safety of the mucosal rDIs vaccine are needed before use in humans. Nonetheless, in this study we demonstrated that it is an effective vector for the induction of Ag-specific mucosal immunity in the mucosally immunized mouse model, and represents an important step towards the development of an effective mucosal rDIs vaccine against HIV.

Acknowledgments

This work was supported by the Human Science Foundation of Japan, and the Japanese Ministry of Health, Labor, and Welfare. A part of this work was supported by the 'Open Research Center' Project for Private Universities: matching fund subsidy from the Ministry of Education, Culture, Sports, Science and Technology, 2004–2008, Iwate Medical University and by a grant from the Keiryokai Research Foundation No. 94.

References

1 Belyakov IM, Wyatt LS, Ahlers JD *et al.* Induction of a mucosal cytotoxic T-lymphocyte response by intrarectal immunization with a replication-deficient recombinant vaccinia virus expressing human immunodeficiency virus 89.6 envelope protein. *J Virol* 1998; 72:8264–72.

2 Amara RR, Villinger F, Altman JD *et al.* Control of a mucosal challenge and prevention of AIDS by a multiprotein DNA/MVA vaccine. *Science* 2001;292:69–74.

3 Casimiro DR, Chen RL, Fu TM *et al.* Comparative immunogenicity in rhesus monkeys of DNA plasmid, recombinant vaccinia virus, and replication-defective adenovirus vectors expressing a human immunodeficiency virus type 1 gag gene. *J Virol* 2003;77:6305–13.

4 Stevceva L, Alvarez X, Lackner AA *et al.* Both mucosal and systemic routes of immunization with the live, attenuated NYVAC/simian immunodeficiency virus SIV_{gpe} recombinant vaccine result in

gag-specific CD8+ T-cell responses in mucosal tissues of macaques. *J Virol* 2002;76:11659–76.
5 Cebere I, Dorrell L, McShane H *et al.* Phase I clinical trial safety of DNA- and modified virus Ankara-vectored human immunodeficiency virus type 1 (HIV-1) vaccines administered alone and in a prime-boost regime to healthy HIV-1-uninfected volunteers. *Vaccine* 2006;24:417–25.
6 Goonetilleke N, Moore S, Dally L *et al.* Induction of multifunctional human immunodeficiency virus type 1 (HIV-1)-specific T cells capable of proliferation in healthy subjects by using a prime-boost regimen of DNA- and modified vaccinia virus Ankara-vectored vaccines expressing HIV-1 Gag coupled to CD8+ T-cell epitopes. *J Virol* 2006;80:4717–28.
7 Jaoko W, Nakwagala FN, Anzala O *et al.* Safety and immunogenicity of recombinant low-dosage HIV-1 A vaccine candidates vectored by plasmid pTHr DNA or modified vaccinia virus Ankara (MVA) in humans in East Africa. *Vaccine* 2008;26:2788–95.
8 Kitamura T, Kitamura Y. Interference with the growth of vaccinia virus by an attenuated mutant virus. *Jpn J Med Sci Biol* 1963;16:343–57.
9 Kitamura T, Kitamura Y, Tagaya I. Immunogenicity of an attenuated strain of vaccinia virus on rabbits and monkeys. *Nature* 1967;215:1187–8.
10 Tagaya I, Kitamura T, Sano Y. A new mutant of dermovaccinia virus. *Nature* 1961;192:381–2.
11 Ishii K, Ueda Y, Matsuo K *et al.* Structural analysis of vaccinia virus DIs strain: application as a new replication-deficient viral vector. *Virology* 2002;302:433–44.
12 Someya K, Xin KQ, Matsuo K, Okuda K, Yamamoto N, Honda M. A consecutive priming-boosting vaccination of mice with simian immunodeficiency virus (SIV) gag/pol DNA and recombinant vaccinia virus strain DIs elicits effective anti-SIV immunity. *J Virol* 2004;78:9842–53.
13 Ami Y, Izumi Y, Matsuo K *et al.* Prime-boost vaccination with recombinant *Mycobacterium bovis* bacillus Calmette-Guérin and a non-replicating vaccinia virus recombinant leads to long-lasting and effective immunity. *J Virol* 2005;79:12871–9.
14 Someya K, Ami Y, Nakasone T *et al.* Induction of positive cellular and humoral immune responses by a prime-boost vaccine encoded with simian immunodeficiency virus gag/pol. *J Immunol* 2006;176:1784–95.
15 Kiyono H, Czerkinsky C. Consideration of mucosally induced tolerance in vaccine development. In: Kiyono H, Ogra PL, McGhee JR, eds. *Mucosal Vaccine*. San Diego: Academic Press, 1996:89–101.
16 Jackson RJ, Fujihashi K, Xu-Amano J, Kiyono H, Elson CO, McGhee JR. Optimizing oral vaccines: induction of systemic and mucosal B-cell and antibody responses to tetanus toxoid by use of cholera toxin as an adjuvant. *Infect Immun* 1993;61:4272–9.
17 Moldoveanu Z, Fujihashi K. Collection and processing of external secretions and tissues of mouse origin. In: Mestecky J, Lamm ME, McGhee JR, Bienenstock J, Mayer L, Strober W, eds. *Mucosal Immunology*, 3rd Edn. San Diego: Academic Press, 2005:1841–52.
18 Unger RE, Marthas ML, Lackner AA *et al.* Detection of simian immunodeficiency virus DNA in macrophages from infected rhesus macaques. *J Med Primatol* 1992;21:74–81.
19 Kempe CH. Studies smallpox and complications of smallpox vaccination. *Pediatrics* 1960;26:176–89.
20 Fulginiti VA, Papier A, Lane JM, Neff JM, Henderson DA. Smallpox vaccination: a review, part II adverse events. *Clin Infect Dis* 2003;37:251–71.
21 Goldstein JA, Neff JM, Lane JM, Koplan JP. Smallpox vaccination reactions, prophylaxis, and therapy of complications. *Pediatrics* 1975;55:342–7.
22 Angulo JJ, de Campos EP, de Gomes LF. Postvaccinal meningoencephalitis; Isolation of the virus from the brain. *J Am Med Assn* 1964;187:151–3.
23 Gurvich EB, Movsesyants AA, Stepenenkova LP. Isolation of vaccinia virus from children with postvaccinal encephalitis at late intervals after vaccination. *Acta Virol* 1975;19:92.
24 Quiding M, Nordström I, Kilander A *et al.* Intestinal immune responses in humans. Oral cholera vaccination induces strong intestinal antibody responses and interferon-gamma production and evokes local immunological memory. *J Clin Invest* 1991;88:143–8.
25 Kozlowski PA, Cu-Uvin S, Neutra MR *et al.* Comparison of the oral, rectal, and vaginal immunization routes for induction of antibodies in rectal and genital tract secretions of women. *Infect Immun* 1997;65:1387–94.
26 Johansson EL, Bergquist C, Edebo A *et al.* Comparison of different routes of vaccination for eliciting antibody responses in the human stomach. *Vaccine* 2004;22:984–90.
27 Johansson EL, Wassén L, Holmgren J *et al.* Nasal and vaginal vaccinations have differential effects on antibody responses in vaginal and cervical secretions in humans. *Infect Immun* 2001;69:7481–6.
28 Vaerman JP, Langendries A, Giffroy D *et al.* Lack of SC/pIgR-mediated epithelial transport of a human polymeric IgA devoid of J chain: *in vitro* and *in vivo* studies. *Immunology* 1998;95:90–6.
29 Meckelein B, Externest D, Schmidt MA *et al.* Contribution of serum immunoglobulin transudate to the antibody immune status of murine intestinal secretions: influence of different sampling procedures. *Clin Diagn Lab Immunol* 2003;10:831–4.
30 Brandtzaeg P. Induction of secretory immunity and memory at mucosal surfaces. *Vaccine* 2007;25:5467–84.
31 Chen PJ, Wang JT, Hwang LH *et al.* Transient immunoglobulin M antibody response to hepatitis C virus capsid antigen in posttransfusion hepatitis C: putative serological marker for acute viral infection. *Proc Natl Acad Sci USA* 1992;89:5971–5.
32 Sjogren M, Hoofnagle JH. Immunoglobulin M antibody to hepatitis B core antigen in patients with chronic type B hepatitis. *Gastroenterology* 1984;89:252–8.
33 Nardelli-Haefliger D, Wirthner D, Schiller JT *et al.* Specific antibody levels at the cervix during the menstrual cycle of women vaccinated with human papillomavirus 16 virus-like particles. *J Natl Cancer Inst* 2003;95:1128–37.

Journal of General Virology (2008), 89, 554–566 DOI 10.1099/vir.0.83186-0

Impact of glycosylation on antigenicity of simian immunodeficiency virus SIV239: induction of rapid V1/V2-specific non-neutralizing antibody and delayed neutralizing antibody following infection with an attenuated deglycosylated mutant

Chie Sugimoto,[1,2,3] Emi E. Nakayama,[4] Tatsuo Shioda,[4] Francois Villinger,[5] Aftab A. Ansari,[5] Naoki Yamamoto,[1] Yasuo Suzuki,[3,6] Yoshiyuki Nagai[7] and Kazuyasu Mori[1,2,3]

Correspondence
Kazuyasu Mori
mori@nih.go.jp

[1]AIDS Research Center, National Institute of Infectious Diseases, Shinjuku-ku, Tokyo 162-8640, Japan

[2]Tsukuba Primate Research Center, National Institute of Biomedical Innovation, Tsukuba, Ibaraki 305-0843, Japan

[3]CREST, Japan Science and Technology Agency, Kawaguchi, Saitama 332-0012, Japan

[4]Department of Viral Infections, Research Institute for Microbial Diseases, Osaka University, Suita, Osaka 565-0871, Japan

[5]Department of Pathology and Laboratory Medicine, Emory University, Atlanta, GA 30322, USA

[6]Department of Biomedical Sciences, College of Life and Health Sciences, Chubu University, Kasugai, Aichi 487-8501, Japan

[7]Center of Research Network for Infectious Diseases, Riken, Chiyoda-ku, Tokyo 100-0006, Japan

Infection of rhesus macaques with a deglycosylation mutant, Δ5G, derived from SIV239, a pathogenic clone of simian immunodeficiency virus (SIV), led to robust acute-phase viral replication followed by a chronic phase with undetectable viral load. This study examined whether humoral responses in Δ5G-infected animals played any role in the control of infection. Neutralizing antibodies (nAbs) were elicited more efficiently in Δ5G-infected animals than in SIV239-infected animals. However, functional nAb measured by 90 % neutralization was prominent in only two of the five Δ5G-infected animals, and only at 8 weeks post-infection (p.i.), when viral loads were already below 10^4 copies ml^{-1}. These results suggest a minimal role for nAbs in the control of the primary infection. In contrast, whilst Ab responses to epitopes localized to the variable loops V1/V2 were detected in all Δ5G-infected animals at 3 weeks p.i., this response was associated with a concomitant reduction in Ab responses to epitopes in gp41 compared with those in SIV239-infected animals. These results suggest that the altered surface glycosylation and/or conformation of viral spikes induce a humoral response against SIV that is distinct from the response induced by SIV239. More interestingly, whereas V1/V2-specific Abs were induced in all animals, these Abs were associated with vigorous Δ5G-specific virion capture ability in only two Δ5G-infected animals that exhibited a functional nAb response. Thus, whereas the deglycosylation mutant infection elicited early virion capture and subsequent nAbs, the responses differed among animals, suggesting the existence of host factors that may influence the functional humoral responses against human immunodeficiency virus/SIV.

Received 25 May 2007
Accepted 7 October 2007

INTRODUCTION

The precise role of antibody (Ab) responses in the containment of human immunodeficiency virus (HIV) remains a subject of intense study and debate. Besides the classical direct virus neutralization properties, antibodies are also capable of blocking infection via other pathways such as antibody-dependent complement-mediated inactivation of virus (Aasa-Chapman *et al.*, 2005) and antibody-dependent cellular lysis (Ahmad & Menezes, 1996; Forthal *et al.*, 2001). Acquiring an understanding of these various mechanisms for their exploitation in the

0008-3186 © 2008 SGM Printed in Great Britain

development of candidate vaccines has been a major challenge.

The envelope protein (Env) of HIV/simian immunodeficiency virus (SIV) comprises an exterior protein (gp120) and a transmembrane (TM) protein (gp41), and trimers of the gp120/gp41 complexes form viral spikes that promote binding to receptors and co-receptors on the cell membrane for entry into the target cells (Wyatt & Sodroski, 1998). The major viral receptors of HIV/SIV include CD4 and a variety of co-receptors such as CCR5 or CXCR4. One desirable target epitope for neutralizing antibody (nAb) that shows relative conservation across clades is the binding site for the co-receptor (Burton *et al.*, 2004; Zolla-Pazner, 2004); however, this site is conformationally cryptic within the viral spike up until immediately after binding of the viral spike to CD4, providing an effective shielding mechanism to the virus. Another distinct feature of HIV/SIV Env is the extensive glycosylation that also effectively prevents access to antibodies directed at the epitopes (Chen *et al.*, 2005; Wyatt & Sodroski, 1998; Wyatt *et al.*, 1998). The gp120 protein possesses 18–33 Asn–X–Ser/Thr sequences, signals for the attachment of *N*-linked carbohydrate side chains (Leonard *et al.*, 1990; Ohgimoto *et al.*, 1998; Regier & Desrosiers, 1990; Zhang *et al.*, 2004). As the carbohydrate moiety is generally weakly immunogenic and is recognized to a large extent as self by the host immune system, the massive glycans on the surface of viral spikes constitute an immunologically silent facade (Wyatt & Sodroski, 1998; Wyatt *et al.*, 1998). As a result, mature viral spikes are protected from nAb and other host immune responses by a massive carbohydrate 'glycan shield' (Chen *et al.*, 2005; Wyatt & Sodroski, 1998; Wyatt *et al.*, 1998). In fact, a prominent role of carbohydrates of HIV/SIV in evasion from immune surveillance has been reported previously as follows. Variants of SIV that have evolved to acquire additional glycans in the variable regions of Env have increased neutralization resistance compared with the parental virus (Chackerian *et al.*, 1997; Cheng-Mayer *et al.*, 1999). Similarly, the appearance of neutralization escape mutants has been associated with altered glycosylation in HIV-1 evolved during the course of infection (Wei *et al.*, 2003). Conversely, infection with SIV239 mutants with deglycosylated Env (lacking *N*-linked glycosylation sites) in the variable loops V1/V2 of gp120 elicited markedly increased titres of nAb (Reitter *et al.*, 1998). We have reported that a deglycosylation mutant, Δ5G, lacking *N*-linked glycosylation sites at aa 79, 146, 171, 460 and 479 in gp120 of SIV239 displayed an attenuated phenotype when used to infect rhesus macaques (Mori *et al.*, 2001; Ohgimoto *et al.*, 1998). In addition, animals infected with Δ5G exhibited almost sterile protection against rechallenge with SIV239 (Mori *et al.*, 2001).

Thus, we suggest that studies aimed at identifying the mechanisms underlying the early and potent immune control of deglycosylated SIV may provide knowledge for the formulation of effective HIV/SIV vaccines. Studies performed herein were therefore directed at attempts to define more precisely the early humoral responses (both virus-specific nAb and non-nAb) generated after infection with Δ5G in rhesus macaques and to compare these responses with those observed in macaques inoculated with wild-type SIV239, with the rationale that results from such studies may help to identify their potential contribution towards viral control of primary infection.

METHODS

Viruses. The molecular pathogenic clone of SIV239 (Regier & Desrosiers, 1990) and its derived deglycosylated mutant, Δ5G, were used in this study. Δ5G was derived by mutagenesis of an SIV239 infectious DNA clone so that the asparagine residues for *N*-glycosylation at aa 79, 146, 171, 460 and 479 in gp120 were converted to glutamine residues (Fig. 1a) (Ohgimoto *et al.*, 1998). Viral stocks of SIV239 and Δ5G were prepared as reported previously (Mori *et al.*, 2001).

Peptides. A series of 72 consecutive 25 mer peptides overlapping by 13 aa were synthesized based on the entire SIV239 Env sequence (Env-1–72). These peptides were synthesized by the Microchemical Facility, Emory University School of Medicine, Atlanta, USA. Another set of 15 mer peptides overlapping by 11 aa around the V1/V2 region in gp120 (V1V2-1–12) was synthesized by Sigma-Aldrich Japan based on the Δ5G sequence (see Fig. 5b). All peptides were dissolved in DMSO diluted in PBS.

Animal infection. Juvenile rhesus macaques originating from Myanmar (Burma) (Mm12, Mm13, Mm20, Mm23 and Mm26) or from Laos (Mm07, Mm22 and Mm25) were used following the results of screening for SIV, simian T-cell lymphotropic virus, B virus and type D retrovirus infection, which were all negative prior to inception of the study. All animals were housed in individual cages and maintained according to the rules and guidelines for experimental animal welfare as outlined by the National Institute of Infectious Diseases and National Institute of Biomedical Innovation. Animals were infected intravenously with Δ5G or SIV239 as described previously (Mori *et al.*, 2001).

Plasma viral load measurements. SIV infection was monitored by measuring the plasma viral RNA load using a highly sensitive quantitative real-time RT-PCR. Viral RNA was isolated from plasma samples from infected animals using a commercial viral RNA isolation kit (Roche Diagnostics). SIV *gag* RNA was amplified and quantified using a method originally developed by Hofmann-Lehmann *et al.* (2000) using a TaqMan EZ RT-PCR kit (Applied Biosystems). The detection sensitivity of plasma viral RNA by this method was 100 viral RNA copies per ml plasma (given as copies ml^{-1}).

Neutralization assay. SIV neutralization was tested according to a protocol using CEMx174/SIVLTR-SEAP cells, originally described by Means *et al.* (1997). To measure low levels of nAb, IgG was purified from plasma as described below and concentrated virus stocks were used.

Anti-gp120 Ab ELISA and anti-Env peptide ELISA. Recombinant SIV239 gp120 and Δ5G gp120 were expressed utilizing a Sendai virus vector as described previously (Mori *et al.*, 2005; Yu *et al.*, 1997). Culture supernatant containing approximately 2 μg secreted SIV gp120 ml^{-1} was diluted with an equal amount of PBS, dispensed into each well of an ELISA plate and allowed to incubate at 4 °C overnight.

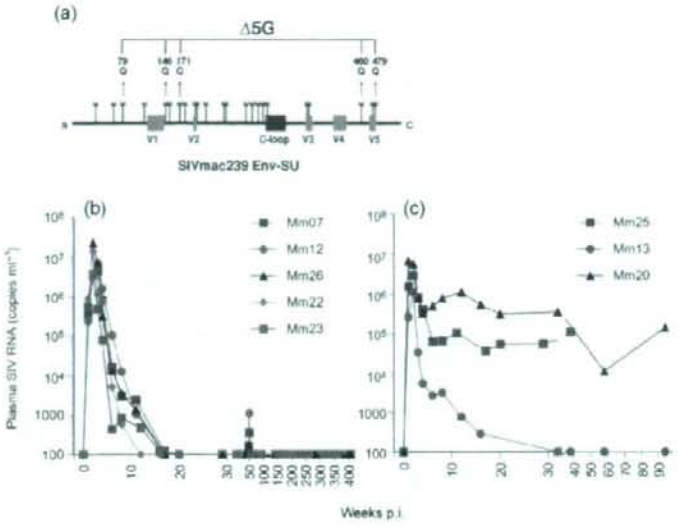

Fig. 1. Plasma SIV RNA loads in animals infected with Δ5G or SIV239. (a) *N*-Glycosylation sites in SIV239 gp120 and deglycosylation sites in Δ5G gp120. The locations of 23 *N*-glycosylation sites in SIV239 gp120, variable regions (V1–V5) and cysteine loops (C-loop) are shown. Δ5G was deglycosylated by N→Q substitutions at aa 79, 146, 171, 460 and 479 in Env (Ohgimoto *et al.*, 1998). (b, c) Plasma viral load in Δ5G-infected (b) and SIV239-infected (c) animals was measured in plasma samples using sensitive real-time RT-PCR to indicate when viral loads declined below 100 copies ml^{-1}. Three Δ5G-infected animals (Mm07, Mm12 and Mm26) were challenged with SIV239 at 48 weeks p.i.; thus, slightly increased viral loads were detected in those animals during weeks 49–51 p.i. (Mori *et al.*, 2001).

For the peptide ELISA, each peptide was diluted to 0.5 μM with 50 mM carbonate buffer (pH 9.5) and captured on Nunc Immobilizer amino plates (Nalge Nunc) at 4 °C overnight. A 1:100 dilution (150 μl) of the plasma sample to be tested was dispensed into antigen-immobilized plates and incubated at 37 °C for 1 h. Ab responses were detected using peroxidase-conjugated goat anti-monkey IgG and *o*-phenylenediamine. Absorbance was measured at 490 nm.

Removal of linear V1/V2 epitope-specific Abs from IgG fractions. A mixture of the peptides (V1V2-9, -10 and -11; see Fig. 5b) was conjugated to a HiTrap NHS-activated HP column (GE Healthcare). IgGs from plasma samples were fractionated using a mAb trap kit (GE Healthcare) and applied to the peptide-conjugated column. The flow-through fractions devoid of anti-V1V2-9, -10 and -11 peptide-specific Abs were collected. The concentration of IgG was determined using a protein assay kit (Bio-Rad).

Virion capture assay. The virion capture assay was modified using a method reported by Nyambi *et al.* (1998). ELISA plates were coated with the IgG samples described above at a concentration of 20 μg ml^{-1} in 50 mM carbonate buffer (pH 9.5) and incubated at 4 °C for 48 h. The plates were washed three times with PBS and blocked with 3% BSA in PBS at 37 °C for 1 h. The plates were then washed three times with serum-free RPMI 1640. Δ5G or SIV239 virion solutions with a $p27^{gag}$ concentration of 15, 7.5 and 3.75 ng in 10% fetal bovine serum/RPMI 1640 were added to each well of the IgG-coated plate and incubated at 37 °C for 3 h. The wells were washed five times with serum-free RPMI 1640 to remove unbound virus. The virus bound to IgG was lysed using MagNA Pure LC Lysis/Binding Buffer (Roche Diagnostics). The viral lysates were subjected to viral RNA purification using a MagNA Pure Compact nucleic acid purification kit (Roche Diagnostics). The copy number of the isolated SIV RNA was determined by real-time RT-PCR for SIV239 as described above.

Statistical analysis. Correlation analysis was done using Spearman's non-parametric rank test and the Mann–Whitney test using GraphPad Prism 4.0 software. Correlations were considered to be statistically significant for values of $P<0.05$.

RESULTS

Plasma viral loads of a quintuple deglycosylated SIV239 mutant in rhesus macaques

Eight rhesus macaques were infected intravenously with Δ5G ($n=5$) or SIV239 ($n=3$) (Mori *et al.*, 2001). Plasma viral RNA loads were assayed for up to 400 weeks p.i. and the data obtained in the Δ5G-infected (Fig. 1b) or SIV239-infected (Fig. 1c) animals were plotted. Both Δ5G and SIV239 replicated with similar kinetics during the early phase of primary infection for up to 4 weeks p.i. However, subsequent to this acute infection phase, virus replication was markedly different in the two groups of monkeys: SIV239-infected animals exhibited viral load set points around 10^5 copies ml^{-1} in two of three animals, with one animal (Mm13) having an undetectable viral load (<100 copies ml^{-1}) by 30 weeks p.i. (Fig. 1c). In contrast, the Δ5G-infected animals showed uniformly controlled viraemia reaching undetectable levels by 12–16 weeks p.i. and maintained this control for more than 6 years p.i. (Fig. 1b).

nAb response in Δ5G-infected animals

Although failure to detect a nAb response is characteristic of SIV239-infected rhesus macaques (Johnson *et al.*, 2003; Means *et al.*, 1997), the rapid control of viraemia in Δ5G-infected animals prompted us to determine whether nAb played a role in this control of viraemia. We hypothesized that the deglycosylation might lead to the elicitation of a markedly more vigorous nAb response than infection with SIV239. To maximize the detection sensitivity of weak nAb responses at early time points p.i., an assay that measures neutralization titres based on 50% inhibition of virus replication (IC_{50}) in $CD4^+$ T-cell lines was initially used.

Consistent with the reported results in SIV239-infected animals, no appreciable nAb titre was detected in two animals (Mm13 and Mm25), despite the fact that viral load in Mm13 was distinctively decreased by 30 weeks p.i. However, we observed a rare animal (Mm20) that elicited a robust nAb response against SIV239 and a relatively delayed nAb response against Δ5G, despite the maintenance of a high viral load (Fig. 2a). These results indicated the lack of correlation of nAb response with viral load in SIV239-infected animals. In contrast, nAb was detected in two Δ5G-infected animals (Mm07 and Mm22) starting at 8 weeks p.i. and in two additional animals (Mm12 and Mm23) at 12 weeks p.i. (Fig. 2b, left panel). These titres peaked at either 12 or 18 weeks p.i., and the peak was followed by a decrease in titre that varied among animals. Mm12 and Mm23, which exhibited nAb induction at 12 weeks p.i., had essentially low titres, whilst Mm07 and Mm22, which exhibited nAb induction at an earlier time point, maintained vigorous nAb titres of >1 : 100. Of note, plasma from Mm26 did not contain detectable levels of nAb at any time p.i. In contrast, nAb against SIV239 was not induced in any of the Δ5G-infected animals (Fig. 2b, right panel). As low-level nAb may play a role in control of virus replication, purified IgG from the plasma samples was used to measure neutralizing activity. However, the results from the purified IgG corresponding to the plasma at a 1 : 3 dilution did not change the kinetics of nAb response in Δ5G-infected animals (data not shown).

In experiments where the passive administration of monoclonal HIV nAb successfully prevented the infection of macaques with simian–human immunodeficiency virus, the results unequivocally indicated that high titres of nAb were needed to achieve such protection (Nishimura *et al.*, 2002). In consideration of these results, data were recalculated based on a cut-off value of 90 % inhibition of virus replication (IC_{90}) in $CD4^+$ T-cell lines. As a result, nAb responses were detected in only two of the animals, Mm07 and Mm22, but with titres of 1 : 100 and 1 : 500, respectively (Fig. 2b, middle panel). Next, we examined the correlation between viral load and nAb titre at 8 and 12 weeks p.i. and found that the correlation was not statistically significant (Fig. 2c).

Anti-gp120 Ab response in Δ5G-infected animals

Next, we measured binding Ab responses against gp120. When the plasma samples were assayed for levels of Ab that bound to SIV239 gp120 or Δ5G gp120, essentially identical values were obtained. Fig. 3 shows the data obtained using SIV239 gp120. Remarkably, anti-gp120 responses during the early period p.i. between the two groups of monkeys were distinct. Whereas anti-gp120-specific Ab responses

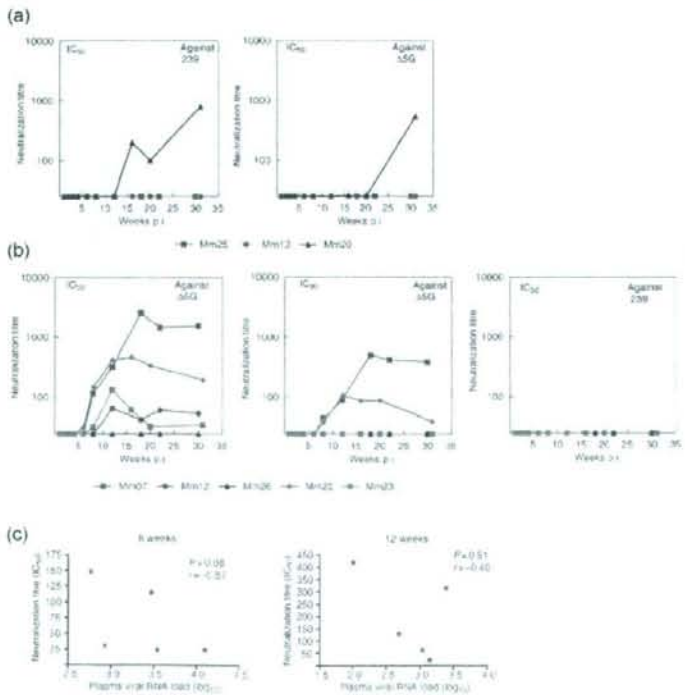

Fig. 2. nAb titres in SIV-infected animals. (a) nAb titres in SIV239-infected animals are indicated as the plasma dilution yielding 50 % inhibition (IC_{50}) of SIV239 infection (left) or Δ5G infection (right) in CEMx174/SIVLTR-SEAP cells. (b) nAb titres in Δ5G-infected animals are indicated as the plasma dilution that yielded 50 % inhibition (IC_{50}, left) and 90 % inhibition (IC_{90}, middle) of Δ5G infection or 50 % inhibition of SIV239 infection (right) in CEMx174/SIVLTR-SEAP cells. (c) Correlation between IC_{50} nAb titres and plasma viral RNA load at 8 and 12 weeks p.i. in Δ5G-infected animals.

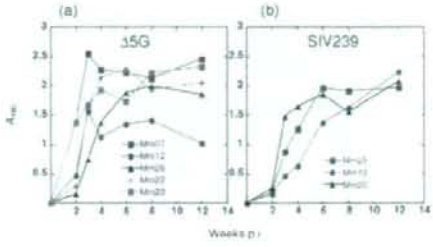

Fig. 3. Anti-gp120 Ab responses. Anti-gp120 Ab responses in Δ5G-infected (a) and SIV239-infected (b) animals were indicated as A_{490} using plasma diluted 1 : 100 in an ELISA.

peaked at 3–4 weeks p.i. in Δ5G-infected animals (Fig. 3a), those in SIV239-infected animals remained generally lower and required longer periods of time to reach their peak (Fig. 3b). Of note, whilst anti-gp120 Ab responses did not correlate well with nAb titres in the chronic phase in Δ5G-infected animals, the hierarchy detected in nAb titres (Mm07, Mm22, Mm23, Mm12 and Mm26, in descending order) was similar to that observed for gp120-binding antibodies at 2 weeks p.i. (Fig. 3a).

Ab responses to linear epitopes in gp120 and gp41 in Δ5G-infected animals differ from those detected in SIV239-infected animals

Next, we examined Ab-binding responses to linear epitopes in plasma samples from infected animals at 8 weeks p.i., as both nAb and anti-gp120-binding Ab were detected at this time point (Figs 2 and 3). We used 72 overlapping peptides encompassing the entire Env sequence of SIV239 for the detection of epitope-specific Ab in plasma samples from Δ5G-infected or SIV239-infected animals. As shown in Fig. 4 and Table 1, the plasma samples reacted with the peptides in six regions: two in gp120 and four in gp41. The regions in gp120 resided in the vicinity of V1/V2, designated region 1 (aa 109–193), and at the C terminus, designated region 2 (aa 493–529). Of note, only linear region 1 was directly affected by selected deglycosylation (aa 146 and 171). The regions in gp41 were located in the ectodomain for region 3 (aa 589–625) and region 4 (aa 660–685), and in the cytoplasmic domain for region 5 (aa 721–757) and region 6 (aa 841–879).

Although Ab responses to most of the peptides recognized in the plasma samples from Δ5G-infected animals were similar to those in SIV239-infected animals, a few peptides were recognized by Abs only in samples from Δ5G-infected animals, and Ab reactivity to some peptides was significantly different between the two groups (Fig. 4b, c and Table 1). Firstly, in region 1, whereas five peptides (Env-10, -12, -13, -14 and -15) were recognized by Abs from Δ5G-infected animals, only three peptides (Env-10, -12 and -13) reacted with Abs from SIV239-infected animals (Fig. 4b and c). Peptide Env-10 was detected by Abs from four Δ5G-infected animals, but from only one of the SIV239-infected animals. Similarly, peptides Env-12 and -13 were detected by Abs from five Δ5G-infected animals and two SIV239-infected animals. In contrast, peptides Env-14 and -15 were detected by Abs from Δ5G-infected animals but not SIV239-infected animals. The specificity of Δ5G infection in the reactivity of peptide Env-14 was statistically significant (P=0.0149) (Table 1). Secondly, the reactivity of Ab from Δ5G-infected animals with the peptides in regions 2, 3 and 4 was lower than that recorded with Ab from SIV239-infected animals (Fig. 4b and c). As shown in Table 1, the reduction in Ab reactivity from Δ5G-infected animals to peptide Env-51 (region 3) and peptide Env-56 (region 4) was significant (P=0.014 and 0.0053, respectively); however, the reduction in Ab response in region 2 was not significant. In addition, there were no significant differences in the Ab responses to the peptides in regions 5 and 6 between Δ5G-infected and SIV239-infected monkeys (Fig. 4b, c and Table 1).

A Δ5G-specific linear epitope resides in the region containing the third deglycosylation site (aa 171) between V1 and V2

As region 1 also contained the site of two mutations introduced to limit glycosylation in the Δ5G mutant, we focused additional studies on this region. To identify the Δ5G-specific epitope(s) in region 1, peptide ELISA was performed with 12 newly synthesized shorter peptides based on the Δ5G sequence spanning the V1/V2 region (Fig. 5). Ab reactivity to peptide Env-14 was mapped to peptides V1V2-9–11 (Fig. 5a). Thus, three linear epitopes (encompassed in peptides Env-10, V1V2-3 and V1V2-9–11) were identified within the V1/V2 region (Figs 4 and 5). Whilst two epitopes contained in peptides Env-10 and V1V2-3 were recognized by Ab from both SIV239- and Δ5G-infected animals, the epitope(s) corresponding to peptides V1V2-9–11 was specific to Δ5G infection (Fig. 5a). As the latter contained the third deglycosylation mutation (Figs 1 and 5b, aa 171), Δ5G specificity was probably secondary to the removal of *N*-glycan at this site in SIV239 gp120 (Fig. 5).

Δ5G-specific Ab responses to linear epitopes in Env elicited immediately following primary infection

In an effort to define the potential relevance of the linear epitope-specific Ab responses in the reduction of acute virus replication in Δ5G-infected animals, we examined the kinetics of Ab reactivity to 12 peptides: Env-10, V1V2-3 and V1V2-9, -10 and -11 for epitopes in region 1; Env-42 and -43 for epitopes in region 2; Env-50 and -51 for epitopes in region 3; Env-56 for epitopes in region 4; and Env-61 and -62 for epitopes in region 5 (Fig. 6). Whilst the induction kinetics of Ab to most peptides were variable in

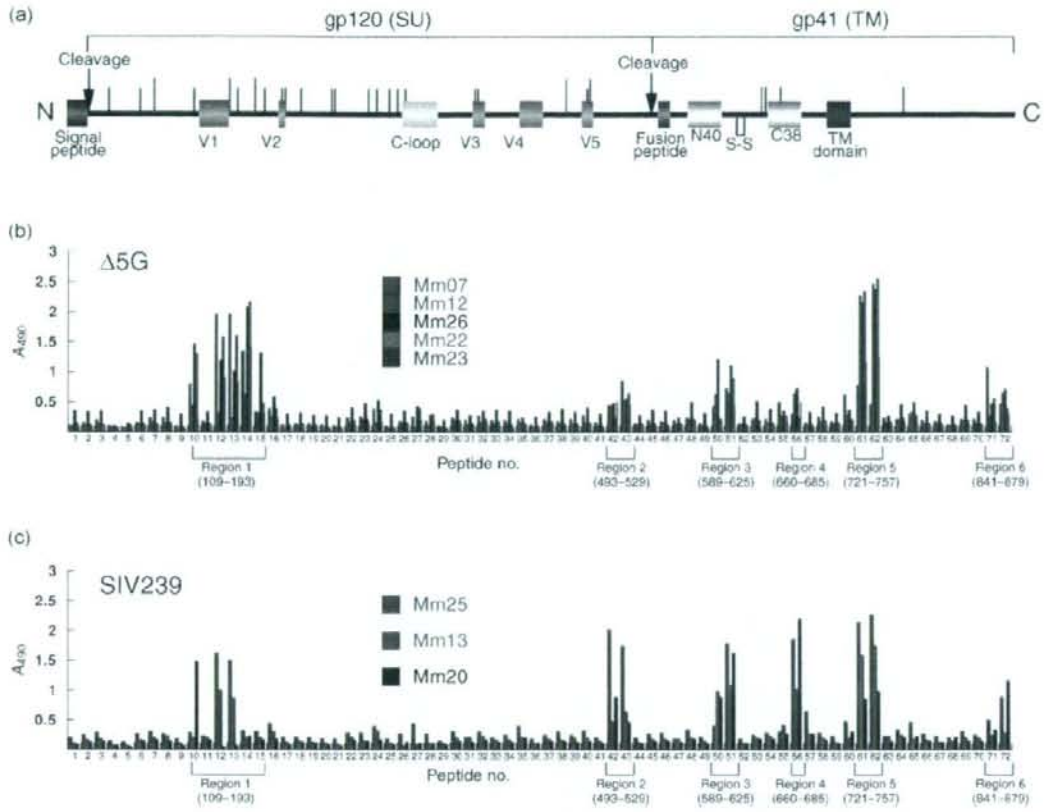

Fig. 4. Ab reactivity to synthetic overlapping peptides spanning the entire Env protein. (a) Diagram of SIV239 Env with the locations of the signal peptide (violet box), variable regions (pink boxes), cysteine loop (yellow box), fusion peptide (green box), N-terminal (N40) and C-terminal (C38) heptad repeats (light-blue boxes), membrane-spanning domain (blue box) and *N*-glycosylation sites (vertical bars) (Burns & Desrosiers, 1991; Choi *et al.*, 1994; Liu *et al.*, 2002). Red vertical bars indicate deglycosylation sites (aa 79, 146, 171, 460 and 479) in Δ5G. S-S indicates the indispensable disulfide bond for hairpin loop formation of the TM protein. (b, c) Plasma samples collected from animals infected with Δ5G (b) and SIV239 (c) at 8 weeks p.i. were used to examine Ab reactivity to 72 peptides (25 mers) overlapping by 13 residues each and spanning the entire Env protein. Reactivity was shown by A_{490}.

plasma from both groups of animals, Ab to V1V2-9, -10 and -11 was specific for Δ5G-infected animals, with rapid induction following primary infection. Ab responses to Env-61 and -62 were also induced rapidly in animals from the two groups; however, it has already been confirmed by SIV and HIV studies that a linear epitope covered by these peptides is the immunodominant epitope with no association with virus control (Eberle *et al.*, 1997; Kent *et al.*, 1992). In contrast to Ab responses to V1/V2 peptides, whilst Ab to peptides Env-51 and -56 in the gp41 ectodomain were detected in SIV239-infected animals, these reactions were low until at least 12 weeks p.i. in Δ5G-infected animals.

Properties of Ab against Δ5G-specific linear epitope

Although Ab reactivity to peptide V1V2-9, -10 and -11 was elicited specifically in Δ5G-infected animals, these Abs were non-nAbs, as these binding Abs were detected in all Δ5G-infected animals, including a nAb-undetectable monkey (Mm26), and before nAb was detected. In addition, we attempted to inhibit neutralization by the addition of excess concentrations of V1V2-9, -10 and -11 to the neutralization assay performed with plasma from Δ5G-infected animals collected at 8 and 12 weeks p.i. The reduction of nAb by the addition of an excess amount of